Title

Integrin α9β1 in airway smooth muscle suppresses exaggerated airway narrowing

Journal

Journal of Clinical Investigation, 122(8)

ISSN

0021-9738

Authors

Chen, Chun
Kudo, Makoto
Rutaganira, Florentine
et al.

Publication Date

2012-08-01

DOI

10.1172/jci60387

Peer reviewed

Integrin $\alpha_9\beta_1$ in airway smooth muscle suppresses exaggerated airway narrowing

Chun Chen,[1] Makoto Kudo,[1] Florentine Rutaganira,[2] Hiromi Takano,[1] Candace Lee,[1] Amha Atakilit,[1] Kathryn S. Robinett,[3] Toshimitsu Uede,[4] Paul J. Wolters,[1] Kevan M. Shokat,[2] Xiaozhu Huang,[1] and Dean Sheppard[1]

[1]Lung Biology Center, Department of Medicine, and [2]Howard Hughes Medical Institute and Department of Cellular and Molecular Pharmacology, UCSF, San Francisco, California, USA. [3]Cardiopulmonary Genomics Program, Department of Medicine, University of Maryland School of Medicine, Baltimore, Maryland, USA. [4]Division of Molecular Immunology, Institute for Genetic Medicine, Hokkaido University, Sapporo, Japan.

Exaggerated contraction of airway smooth muscle is the major cause of symptoms in asthma, but the mechanisms that prevent exaggerated contraction are incompletely understood. Here, we showed that integrin $\alpha_9\beta_1$ on airway smooth muscle localizes the polyamine catabolizing enzyme spermidine/spermine N^1-acetyltransferase (SSAT) in close proximity to the lipid kinase PIP5K1γ. As PIP5K1γ is the major source of PIP2 in airway smooth muscle and its activity is regulated by higher-order polyamines, this interaction inhibited IP3-dependent airway smooth muscle contraction. Mice lacking integrin $\alpha_9\beta_1$ in smooth muscle had increased airway responsiveness in vivo, and loss or inhibition of integrin $\alpha_9\beta_1$ increased in vitro airway narrowing and airway smooth muscle contraction in murine and human airways. Contraction was enhanced in control airways by the higher-order polyamine spermine or by cell-permeable PIP2, but these interventions had no effect on airways lacking integrin $\alpha_9\beta_1$ or treated with integrin $\alpha_9\beta_1$–blocking antibodies. Enhancement of SSAT activity or knockdown of PIP5K1γ inhibited airway contraction, but only in the presence of functional integrin $\alpha_9\beta_1$. Therefore, integrin $\alpha_9\beta_1$ appears to serve as a brake on airway smooth muscle contraction by recruiting SSAT, which facilitates local catabolism of polyamines and thereby inhibits PIP5K1γ. Targeting key components of this pathway could thus lead to new treatment strategies for asthma.

Introduction

Asthma is characterized by exaggerated narrowing of the conducting airways of the lung in response to normally trivial bronchoconstrictor stimuli. Airway narrowing in asthma is largely dependent on contraction of airway smooth muscle. However, the pathways that regulate airway smooth muscle contraction are incompletely understood.

Integrins are a family of transmembrane heterodimers that participate in the translation of spatially fixed extracellular signals into a wide variety of changes in cell behavior (1, 2). Members of this family share a number of common functions (e.g., cell attachment, spreading, and survival) and use a number of common signaling intermediates (e.g., the focal adhesion kinase and src family kinases) (2, 3). However, the diverse and largely nonoverlapping phenotypes of lines of mice expressing KO alleles of individual integrin subunit genes underscore the biological importance of integrin specificity (4–7). Several integrins have been shown to modulate allergic asthma, including $\alpha_4\beta_1$ (8–10), $\alpha_L\beta_2$ (11), $\alpha_v\beta_6$ (12), and $\alpha_v\beta_8$ (13), through effects on leukocyte recruitment, mast cell protease modulation, and modulation of T cell cytokine production. Multiple integrins have been shown to be expressed on airway smooth muscle, where they can modulate cell proliferation and have been proposed to affect airway smooth muscle contraction, in vitro, through modulating connections between the contractile apparatus and the underlying ECM (14). Recent studies have shown that sequence variants in integrins or related genes, such as integrin β_3 (15) or ADAM33 (16), are associated with asthma and allergic disease, but to date, no studies to our knowledge have demonstrated important roles for airway smooth muscle integrins in vivo.

Our lab previously showed that integrin $\alpha_9\beta_1$ is highly expressed in airway smooth muscle: mice constitutively lacking integrin α_9 (encoded by *Itga9*) all die by 12 days of age from respiratory failure (17). To study the role of this integrin in airway smooth muscle function, we generated mice lacking integrin α_9 only in smooth muscle and used them to examine how integrin $\alpha_9\beta_1$ regulates airway smooth muscle function.

Results

Loss of integrin α_9 in smooth muscle causes spontaneous airway hyperresponsiveness in vivo. We generated mice with a knockin of β-gal (*LacZ*) into the endogenous *Itga9* locus to study integrin α_9 expression in the mouse lung. We counterstained with antibody against E-cadherin and α-SMA to identify smooth muscle and distinguish airway from vascular smooth muscle (adjacent to and distant from E-cadherin staining, respectively). This confirmed that integrin $\alpha_9\beta_1$ was highly expressed in airway smooth muscle, but not vascular smooth muscle (Figure 1A). We generated mice with specific KO of integrin α_9 in smooth muscle (referred to herein as $\alpha_9$smKO mice) by crossing *Itga9*$^{fl/fl}$ mice (18) with mice expressing the reverse tetracycline transactivator under the control of the α-SMA promoter (α-sm-rTTA) and (tetO)7-cre (19). Because integrin α_9 was not expressed in vascular smooth muscle in the lungs, it was effectively deleted specifically in airway smooth muscle. Immunohistochemistry confirmed decreased expression of integrin $\alpha_9\beta_1$ in airway smooth muscle (Figure 1B). The high efficiency of recombination in airway smooth muscle was further confirmed by Western blot of primary cultured airway smooth muscle cells (Supplemental Figure 1A; supplemental material available online with this article; doi:10.1172/JCI60387DS1). We evaluated the tissue specificity of recombination in this line by crossing $\alpha_9$smKO

Conflict of interest: The authors have declared that no conflict of interest exists.
Citation for this article: *J Clin Invest.* 2012;122(8):2916–2927. doi:10.1172/JCI60387.

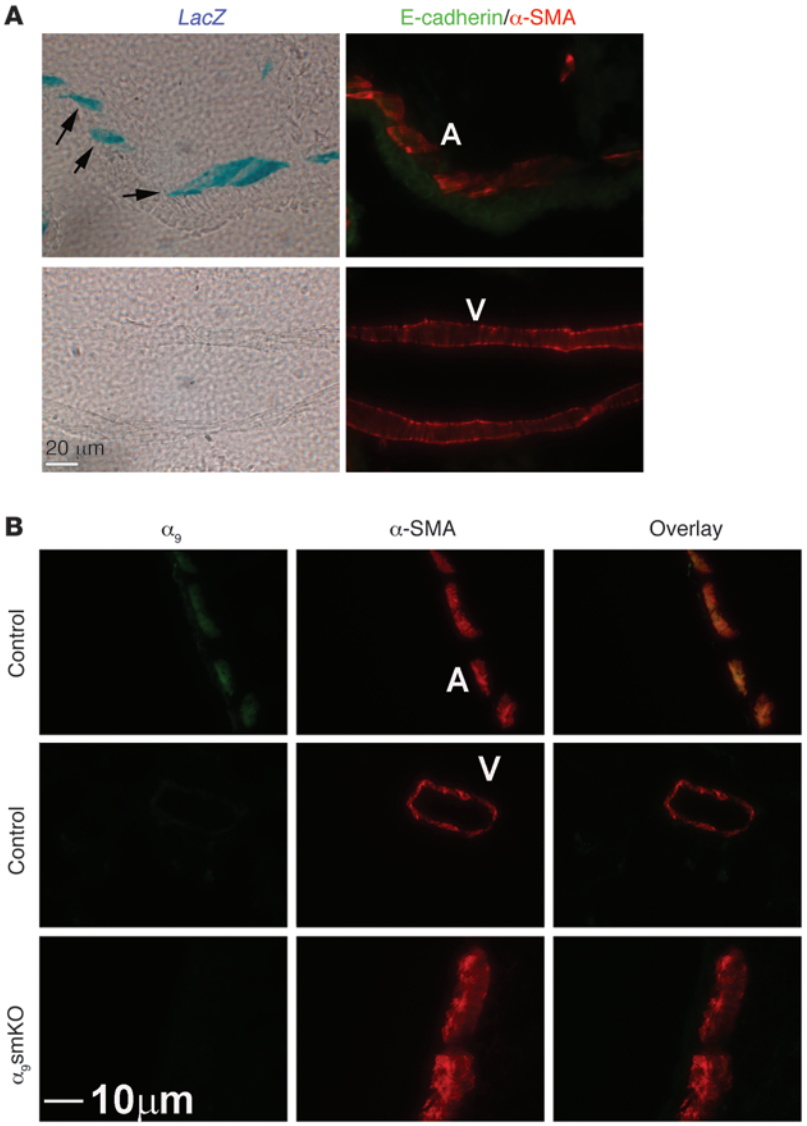

Figure 1
Integrin $\alpha_9\beta_1$ is specifically expressed in airway smooth muscle cells in the mouse lung. (**A**) X-gal staining on 10-μm mouse lung sections from *Itga9 LacZ*-knockin reporter mice. β-gal–positive staining is indicated by arrows. The same section was also used for immunofluorescent staining with anti–E-cadherin (green) and anti–α-SMA (red) to identify airway and vascular smooth muscle (A and V, respectively). (**B**) Immunofluorescence staining of mouse airway and vascular smooth muscle with antibodies against integrin α_9. $\alpha_9$smKO mice had decreased expression in airway smooth muscle. Scale bars: 20 μm (**A**); 10 μm (**B**).

mice with a fluorescent reporter line (20). The mT/mG double-fluorescent Cre reporter line expresses membrane-targeted tandem dimer Tomato (mTomato) prior to Cre-mediated excision and membrane-targeted GFP (mGFP) after excision. Based on the GFP expression in the lung, $\alpha_9$smKO mice demonstrated highly efficient recombination in smooth muscle, which was further confirmed by anti–α-SMA staining (Supplemental Figure 1B).

Airway responsiveness to acetylcholine was measured in anesthetized and paralyzed mechanically ventilated mice. $\alpha_9$smKO mice had significantly increased airway responsiveness (Figure 2A). $\alpha_9$smKO and control mice had comparable lung and airway histology, with no abnormalities in airway epithelium, and there was no evidence of inflammation in $\alpha_9$smKO lungs (data not shown). We assessed static distensibility by measuring static lung compliance and found no difference between $\alpha_9$smKO and control mice (Supplemental Figure 2). There were also no apparent differences in the volume of airway smooth muscle tissue (determined by anti–α-SMA staining) between $\alpha_9$smKO and control mice (data not shown). These findings suggest that the observed differences in airway responsiveness are most likely caused by differences in the function, rather than the structure, of airway smooth muscle. We previously found that heterozygous *Itga9*$^{+/-}$ mice are fully viable and have no detectable morphologic differences from *Itga9*$^{+/+}$ mice (17). However, when we examined airway responsiveness in these animals, they exhibited an intermediate phenotype, with a small but significant increase in airway responsiveness (Figure 2B). This result suggests that even a modest reduction in the level of $\alpha_9\beta_1$ expression can affect airway responsiveness and that the hyperresponsiveness in $\alpha_9$smKO mice is not likely to be caused by overexpression of Cre recombinase or rTTA protein.

Integrin $\alpha_9\beta_1$ inhibits airway narrowing and smooth muscle contraction in vitro. To directly determine whether the differences in pulmonary resistance are due to differences in airway narrowing, we examined ex vivo airway contraction in mouse lung slices, a protocol modified from the one reported by Sanderson's laboratory (21). Airway narrowing was determined by the decrease of lumen area induced by methacholine, as shown in Figure 2C and Supplemental Video 1. Methacholine induced significantly more narrowing in airways from $\alpha_9$smKO than control mice (Figure 2D). There were no differences in the duration of contraction between $\alpha_9$smKO and control animals. To exclude effects caused by genetic compensation, we also induced loss of smooth muscle ex vivo by infecting lung slices prepared from *Itga9*$^{fl/fl}$ mice with adenovirus expressing Cre recombinase. In vitro loss of integrin α_9 induced a very similar and significant increase in airway narrowing (Figure 2E). The high efficiency of recombination in lung slices was further confirmed by Western blot (Supplemental Figure 3). We also incubated lung slices with hamster monoclonal blocking antibody against integrin $\alpha_9\beta_1$ (22); this in vitro inhibition of $\alpha_9\beta_1$ ligation also increased airway narrowing compared with hamster IgG control (Figure 2F).

Loss of integrin α_9 in smooth muscle also increased methacholine-induced in vitro force generation by excised tracheal rings (Figure 3A). As we observed with lung slices, integrin $\alpha_9\beta_1$–blocking antibody or gene deletion ex vivo by infection with adenovirus-Cre increased force generation in response to methacholine (Figure 3, C and E). To determine whether loss of integrin $\alpha_9\beta_1$ ligation on airway smooth muscle specifically enhances signaling through acetylcholine receptors, we examined the effects of integrin $\alpha_9\beta_1$ inhibition on contraction mediated by serotonin (5-HT), which

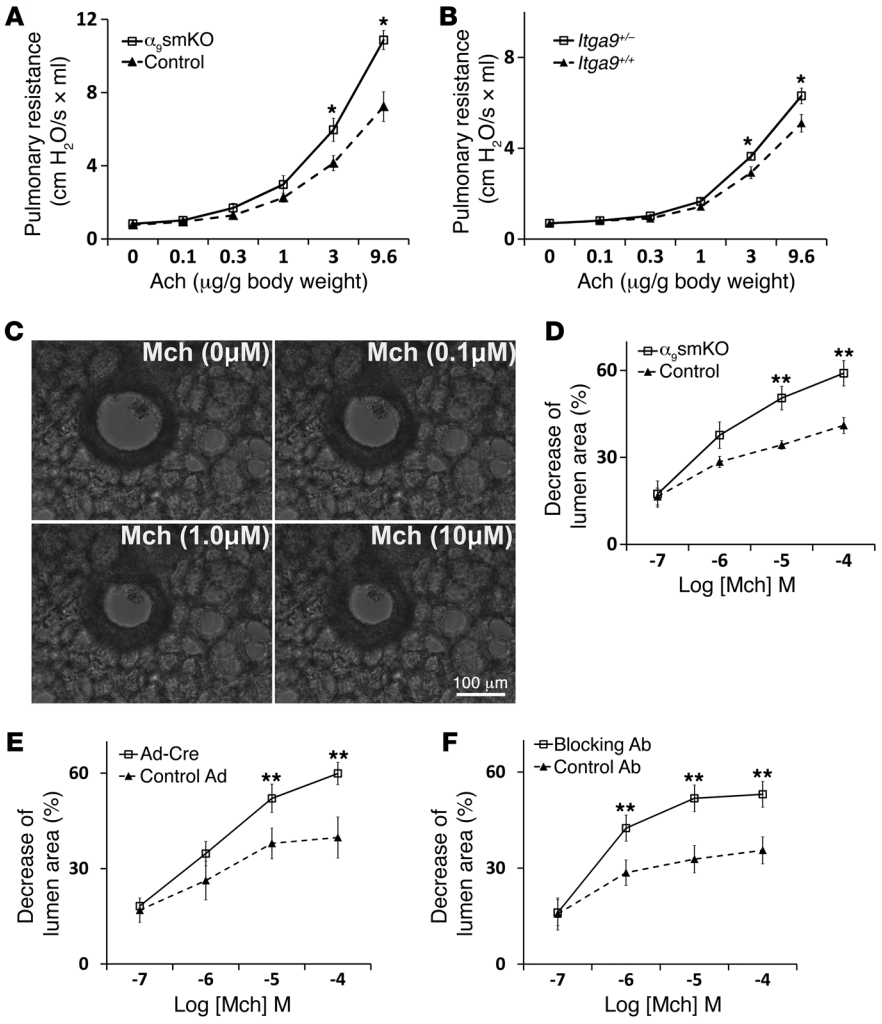

Figure 2

Integrin $\alpha_9\beta_1$ plays a protection role in airway hyperresponsiveness. (**A**) Airway responsiveness to acetylcholine (Ach), measured in anesthetized, ventilated $\alpha_9$smKO mice or littermate controls using a Scireq pulmonary mechanics analyzer. (**B**) Airway hyperresponsiveness in *Itga9*$^{+/-}$ and *Itga9*$^{+/+}$ mice. (**C**) Series of phase-contrast images demonstrating the resting and contractile states of the airway upon exposure to various concentration of methacholine (Mch). Scale bar: 100 μm. (**D**) Airway narrowing in lung slices from WT control or $\alpha_9$smKO mice in response to a range of concentrations of methacholine. (**E**) Airway narrowing in lung slices from *Itga9*$^{fl/fl}$ mice on day 3 after infection with adenovirus expressing Cre recombinase or GFP (as control). (**F**) Airway narrowing in lung slices from WT mice treated in vitro with blocking antibody or control hamster antibody. Results (mean ± SEM) are representative of 3 independent experiments (n = 8). *P < 0.05; **P < 0.01.

induces contraction by activating a separate G protein–coupled receptor (23). Lung slices and tracheal rings from $\alpha_9$smKO mice showed increased contractile responses to 5-HT (Supplemental Figure 4, A and B). Integrin $\alpha_9\beta_1$–blocking antibody also enhanced 5-HT–induced contraction in both mouse lung slices and tracheal rings (Supplemental Figure 4, C and D). 5-HT and cholinergic agonists induce airway smooth muscle contraction by activating PLC, which converts phosphatidylinositol 4,5-bisphosphate (PIP2) to 1,4,5-trisphosphate (IP_3). IP_3 then binds to IP_3 receptors on the sarcoplasmic reticulum (SR) to induce release of calcium into the cytosol, which triggers downstream events that lead to smooth muscle contraction. Alternatively, smooth muscle contraction can be induced by influx of extracellular calcium, for example, by activating voltage-gated calcium channels through addition of extracellular KCl. To determine whether loss of integrin α_9 enhances smooth muscle contraction downstream of changes in intracellular calcium, we examined the effects of integrin $\alpha_9\beta_1$ gene deletion, blocking antibody, and ex vivo deletion by adenovirus-Cre on KCl-induced contraction and found no effect (Figure 3, B, D, and F). To exclude possible nonspecific effects of blocking antibody on cells other than airway smooth muscle, we examined the effects of blocking antibody on $\alpha_9$smKO lung slices and found no further increase in airway narrowing (Supplemental Figure 5).

Tracheal rings contain a number of cell types, including a layer of epithelial cells. To evaluate whether the phenomenon we observed was due to indirect effects through airway epithelial cells, we removed epithelium from tracheal rings. As expected, epithelium removal enhanced the magnitude of force generation in response to methacholine. However, the difference between WT and $\alpha_9$smKO tracheal rings was sustained (Supplemental Figure 6), which suggests that the inhibitory effect of integrin $\alpha_9\beta_1$ on smooth muscle contraction does not depend on effects on epithelial cells. Together, these results suggest that integrin $\alpha_9\beta_1$ regulates airway smooth muscle contraction by modulating the pathway by which activation of G protein–coupled receptors stimulates calcium release.

Integrin α_9–mediated inhibition of airway smooth muscle contraction is mediated by modulation of polyamine catabolism. We have previously shown that the integrin α_9 cytoplasmic domain specifically binds to the polyamine catabolizing enzyme spermidine/spermine N^1-acetyltransferase (SSAT) and that this effect is critical for integrin $\alpha_9\beta_1$–dependent cell migration (24, 25). To determine whether the interaction of the integrin α_9 cytoplasmic domain with SSAT is also important for integrin $\alpha_9\beta_1$–mediated modulation of airway smooth muscle contraction, we evaluated the effects of stabilizing SSAT (and thus effectively enhancing SSAT activity) on airway contraction using the polyamine analog N^1,N^{11}-bis(ethyl)norspermine

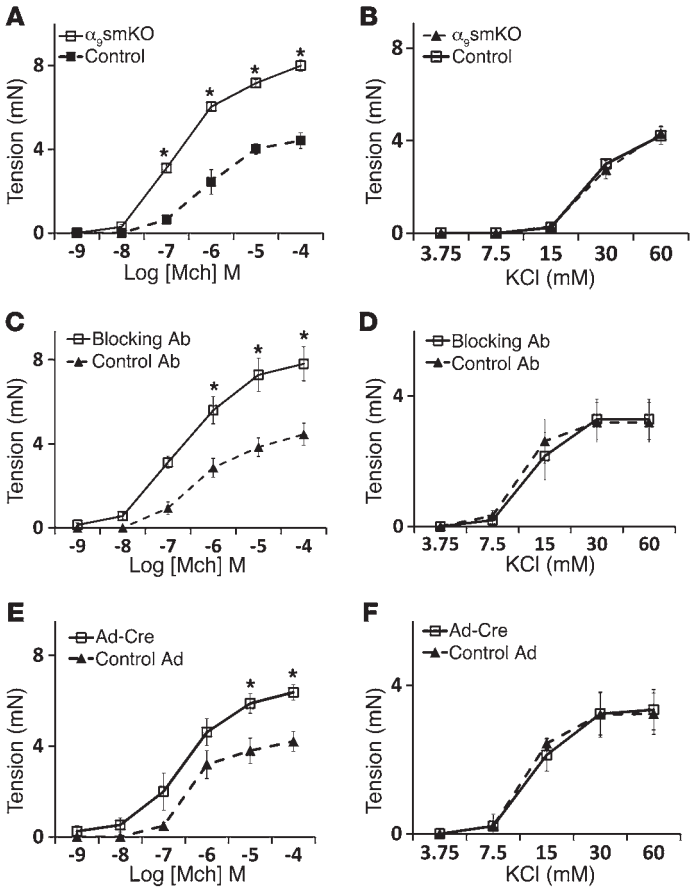

Figure 3
Increased tension generation in tracheal rings from $\alpha_9$smKO mice. (**A** and **B**) Force generation in response to methacholine (**A**) and KCl (**B**) by tracheal rings from WT control or $\alpha_9$smKO mice. (**C** and **D**) Force generation in response to methacholine (**C**) and KCl (**D**) by tracheal rings from WT mice pretreated in vitro with blocking antibody or control antibody. (**E** and **F**) Tracheal rings from *Itga9*$^{fl/fl}$ mice were infected with adenovirus expressing Cre recombinase or GFP (as control) for 3 days before assessment of contractile response to methacholine (**E**) and KCl (**F**). Results (mean ± SEM) are representative of 2 independent experiments (n = 10). *P < 0.01.

tetrahydrochloride (BE3-3-3), which prevents proteasome-mediated SSAT degradation (26). BE3-3-3 inhibited airway contraction in WT lung slices and tracheal rings, but had no effect on the enhanced contraction induced by loss or blockade of integrin α_9 (Figure 4, A–D). These results support the hypothesis that integrin α_9–dependent inhibition of airway smooth muscle contraction depends on the interaction of the integrin α_9 cytoplasmic domain with SSAT.

We next investigated whether the metabolism of polyamines plays a role in integrin $\alpha_9\beta_1$–mediated inhibition of airway narrowing. The oxidative catabolism of the higher-order polyamines, spermidine and spermine, is accomplished by the concerted action of 2 different enzymes, SSAT and polyamine oxidase (PAO). Cytosolic SSAT N^1-acetylates both spermidine and spermine, which then serve as substrates for PAO (27). Because PAO strongly prefers acetylated polyamines to unmodified polyamines as its substrates, SSAT is generally considered the rate-controlling enzyme in the back conversion of the higher-order polyamines spermidine and spermine to the lower-order polyamine putrescine. We thus examined the effects of exogenous spermine (which should compensate for spermine catabolism by SSAT) or exogenous putrescine in order to determine whether integrin $\alpha_9\beta_1$ specifically inhibits airway smooth muscle contraction by reducing concentrations of higher-order polyamines or by increasing the concentration of the end product putrescine. Spermine clearly increased contraction of control lung slices and tracheal rings, but had no effect on $\alpha_9$smKO lung slices or tracheal rings (Figure 5, A–D). Putrescine had no effect on airway contraction. Similar results were also obtained with WT lung slices and tracheal rings treated with polyamines in the presence of integrin α_9–blocking antibody (Supplemental Figure 7). To exclude the possibility that we failed to see additive effects of integrin α_9 loss and spermine treatment because each intervention causes maximal airway narrowing or force generation, we examined the additional effects of another enhancer of airway smooth muscle contraction, IL-13. IL-13 clearly further enhanced contraction in lung slices treated with either blocking antibody or spermine (Supplemental Figure 8, A and B), which suggests that the absence of additive effects of loss or blockade of integrin α_9 and spermine are not the result of either

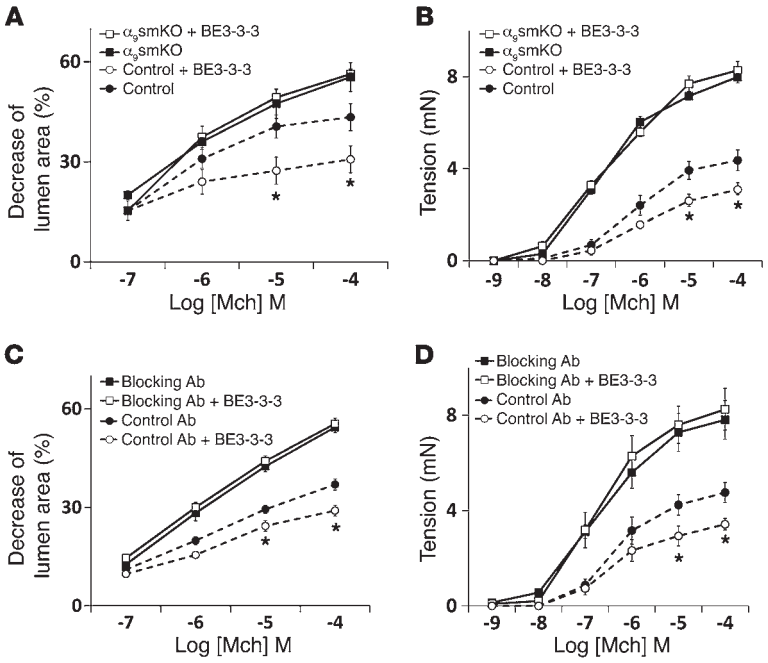

Figure 4
The effect of airway smooth muscle integrin $\alpha_9\beta_1$ depends on SSAT. Airway narrowing in lung slices (**A** and **C**) and tension in tracheal rings (**B** and **D**) from control and $\alpha_9$smKO mice, either (**A** and **B**) untreated or (**C** and **D**) treated with control or blocking antibody, in the presence or absence of 50 μM BE3-3-3 for 24 hours. Results (mean ± SEM) are representative of 2 independent experiments (n = 10). *P < 0.01.

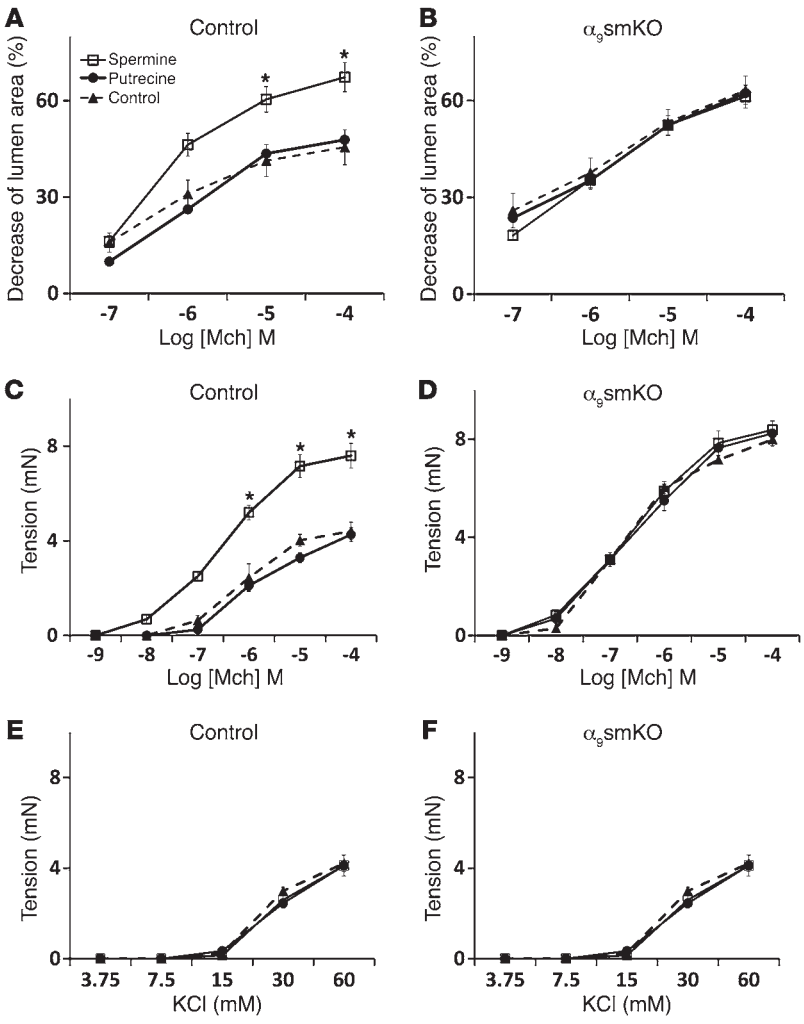

Figure 5
The effect of airway smooth muscle integrin $\alpha_9\beta_1$ depends on polyamine catabolism. Lung slices (**A** and **B**) and tracheal rings (**C**–**F**) from WT control (**A**, **C**, and **E**) or $\alpha_9$smKO (**B**, **D**, and **F**) mice were incubated with polyamines (putrecine or spermine; 100 μM each) for 24 hours before assessment of airway narrowing or tension in response to methacholine (**A**–**D**) or KCl (**E** and **F**). *$P < 0.01$. Results (mean ± SEM) are representative of 2 independent experiments ($n = 10$).

agent inducing maximal contraction. Together, these results are consistent with the hypothesis that integrin $\alpha_9\beta_1$ normally inhibits airway smooth muscle contraction by facilitating local decreases in the concentration of higher-order polyamines.

Integrin $\alpha_9\beta_1$ modulates smooth muscle calcium oscillation frequency and myosin light chain phosphorylation. Our finding that loss of integrin $\alpha_9\beta_1$ enhanced airway smooth muscle contraction in response to cholinergic agonists and 5-HT, but not depolarization by KCl, suggests that this integrin is modulating a pathway downstream of G protein–coupled receptors, but upstream of IP_3-mediated calcium release. Previous studies have shown that G protein–coupled receptor agonists induce cyclic release and reuptake of calcium, leading to cytosolic Ca^{2+} oscillations, and that the magnitude of the resultant smooth muscle contraction is best correlated with the frequency of these Ca^{2+} oscillations (28). To evaluate whether integrin $\alpha_9\beta_1$ modulates airway smooth muscle contraction through effects on Ca^{2+} release, we loaded lung slices with Oregon Green 488 BABTA-1-AM and evaluated Ca^{2+} oscillations at video rate (Supplemental Video 2). Methacholine-induced Ca^{2+} oscillations occurred at markedly higher frequency in slices from $\alpha_9$smKO mice (Figure 6A). The frequency of Ca^{2+} oscillations was increased by spermine treatment and decreased by BE3-3-3 treatment, but only in lung slices from control mice (Figure 6B), completely consistent with our observations for airway contraction. These findings suggest that ligated integrin $\alpha_9\beta_1$ inhibits airway smooth muscle contraction by acting downstream of G protein–coupled receptors, but upstream of Ca^{2+} release from the SR.

Contraction of airway smooth muscle is dependent on activation of actin and myosin cross-bridges and phosphorylation of myosin light chain (MLC) by MLC kinase. The degree to which MLC is phosphorylated can determine the velocity of smooth muscle shortening and maximum contraction (29). We found that methacholine-induced MLC phosphorylation was increased in smooth muscle of $\alpha_9$smKO animals. As above, MLC phosphorylation was inhibited by BE3-3-3 and enhanced by spermine in smooth muscle dissected from control airway tracheal rings, but unaffected by either treatment in smooth muscle from $\alpha_9$smKO mice (Figure 6C).

Integrin $\alpha_9\beta_1$, SSAT, and polyamines have similar roles in human airways. To determine whether the pathway we identified in murine airways is also relevant to airway narrowing in humans, we examined the effects of integrin $\alpha_9\beta_1$ inhibition and of BE3-3-3 and spermine treatment on narrowing of airways in human lung slices and on force generation in human bronchial rings. First, we confirmed that integrin $\alpha_9\beta_1$ was highly expressed in human airway smooth muscle cells by costaining of integrin and α-SMA (Supplemental Figure 9). As we found in murine airways, human airway contraction was increased by integrin $\alpha_9\beta_1$–blocking antibody in both bronchial rings and lung slices (Figure 7, A and E). Human airway contraction was also inhibited by BE3-3-3 and enhanced by spermine (Figure 7, C and F). There were no effects of blocking antibody on KCl-induced contraction (Figure 7, B and D). Overall, these data support an important role of the pathway we describe in human airway smooth muscle and suggest that SSAT could be a potential target for the treatment of asthma.

PIP2 and PIP5K1γ play critical roles in inhibition of smooth muscle contraction by integrin $\alpha_9\beta_1$. One of the best-characterized effects of spermine and spermidine that is not shared by the breakdown product putrescine is dramatic enhancement of the activity of the lipid kinase PIP5K1γ. PIP5K1γ adds a second phosphate to phosphatidylinositol 4-phosphate (PI4P) to generate PIP2 (30) and is the major lipid kinase responsible for generation of PIP2 in airway smooth muscle (31). PIP2 is the essential precursor for IP_3, which, as described above, is generated by PLC in response to G protein–coupled receptor activation and directly mediates cyclic Ca^{2+}

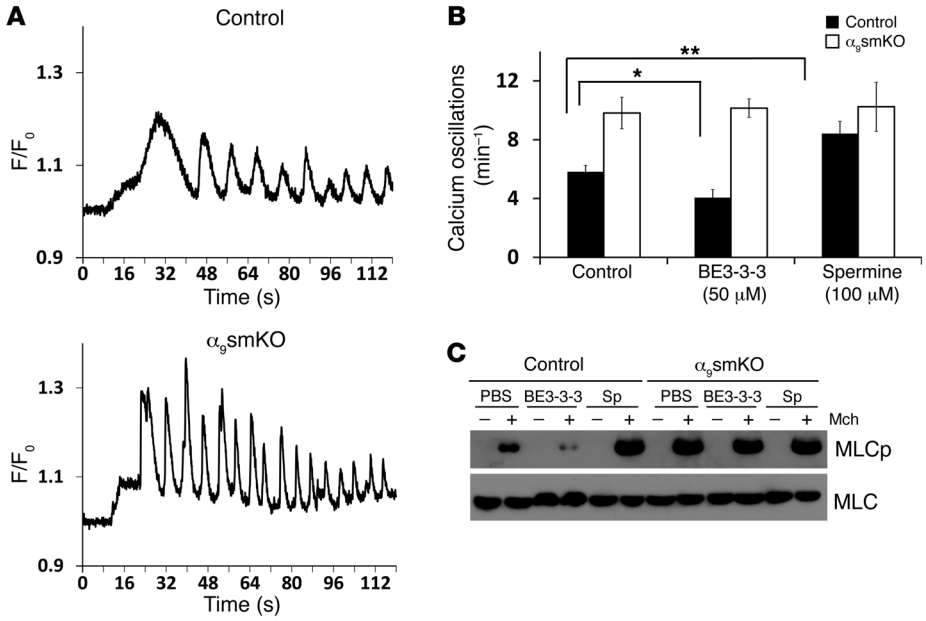

Figure 6
Airway smooth muscle cells in $\alpha_9$smKO lung slices have increased calcium wave and MLC phosphorylation in response to methacholine. (**A**) Representative calcium oscillations induced by 10 μM methacholine in lung slices from WT control and $\alpha_9$smKO mice. Final fluorescence values are expressed as ratios (F/F_0), normalized to the fluorescence immediately prior to the addition of an agonist (F_0). (**B**) Effects of the SSAT stabilizer BE3-3-3 (50 μM) or exogenous spermine (100 μM) on calcium oscillations induced by 10 μM methacholine in lung slices from control or $\alpha_9$smKO mice. Data (mean ± SEM) represent 3 independent experiments with similar results. $^*P < 0.05$; $^{**}P < 0.01$. (**C**) Western blot of total MLC or phosphorylated MLC (MLCp) in lysates enriched for airway smooth muscle dissected from control and $\alpha_9$smKO tracheas treated with or without methacholine (10 μM) in vitro. Sp, spermine.

release from the SR. Importantly, PIP5K1γ is the only lipid kinase with a focal adhesion targeting domain, which has been previously shown to directly bind the focal adhesion protein talin, which in turn binds directly to the cytoplasmic domains of integrin β subunits, including β_1 (32, 33). We therefore hypothesized that integrin $\alpha_9\beta_1$ might inhibit airway smooth muscle contraction by localizing SSAT and locally catabolizing spermine and spermidine, thus decreasing PIP5K1γ activity, reducing local PIP2 production, and resulting in less IP_3 production. If this hypothesis is correct, we should be able to overcome the inhibitory effects of ligated integrin $\alpha_9\beta_1$ by adding excess PIP2. We therefore incubated lung slices with either a cell-permeable form of PIP2 (diC16-PIP2) or its carrier vehicle (carrier 3) and evaluated airway narrowing in response to methacholine. diC16-PIP2 significantly increased airway narrowing in control slices, to the same level seen in slices from untreated $\alpha_9$smKO mice, but had no additional effect in lung slices from $\alpha_9$smKO mice or from mice treated with integrin α_9–blocking antibody (Figure 8, A and B).

We first confirmed that PIP5K1γ was highly expressed in tracheal smooth muscle tissue (Supplemental Figure 10). We then confirmed that PIP5K1γ associates with integrin $\alpha_9\beta_1$ in airway smooth muscle by IP and immunofluorescent staining. IP of integrin α_9 from lysates of WT murine tracheal smooth muscle tissue also precipitated PIP5K1γ (Figure 8C). Integrin α_9 was also found in the complex precipitated by anti-SSAT (Figure 8D). We also found that PIP5K1γ and integrin α_9 colocalized in focal adhesions of cultured murine airway smooth muscle, whereas a mutant form of PIP5K1γ lacking the talin-binding (integrin-targeting) domain did not colocalize with integrin α_9 (Figure 8E). This colocalization was not dependent on PIP5K1γ kinase activity, since kinase-dead PIP5K1γ and integrin α_9 colocalized. To more directly examine the functional significance of PIP5K1γ in these responses, we constructed adenoviruses expressing mcherry-tagged full-length murine PIP5K1γ, a kinase-dead version, or a version expressing a splice variant lacking the talin-binding domain and examined the effects on methacholine-induced contraction of WT lung slices. Full-length PIP5K1γ enhanced airway narrowing, but the kinase-dead version and the version lacking the talin-binding domain did not (Figure 9A). Interestingly, full-length PIP5K1γ did not further enhance airway narrowing in lungs slices treated with integrin $\alpha_9\beta_1$–blocking antibody, whereas the kinase-dead mutant showed a dominant-negative inhibitory effect (Figure 9B). This suggests that in the absence of ligated integrin $\alpha_9\beta_1$, there was sufficient PIP5K1γ present at baseline to saturate the requirement for local PIP2. We also generated adenovirus expressing shRNA for PIP5K1γ. Knockdown efficiency was found to be greater than 90% in mouse fibroblasts (Supplemental Figure 11). Knockdown of PIP5K1γ decreased airway contraction in lung slices in the presence or absence of integrin $\alpha_9\beta_1$–blocking antibody (Figure 9C), which confirmed the important role this enzyme plays in the contractile response to methacholine. Although PIP5K1γ shRNA did not reduce contraction of slices treated with blocking antibody to the level seen with shRNA in WT slices, this partial response is likely explained by incomplete knockdown in lung slices (Figure 9D).

To further test our hypothesis, we measured PIP5K1γ activity by immunoprecipitating the enzyme from lysates of tracheal smooth muscle cells from control and $\alpha_9$smKO mice in the presence of absence of BE3-3-3 or spermine treatment. PIP5K1γ kinase activity was higher in $\alpha_9$smKO than in control smooth muscle (Figure 10A). Activity was increased by spermine and decreased by BE3-3-3 in WT smooth muscle, but neither treatment had any effect in muscle from $\alpha_9$smKO mice (Figure 10B). Overall, these data support the hypothesis that integrin $\alpha_9\beta_1$ and SSAT prevent airway narrowing at least in part through local modulation of PIP5K1γ activity and PIP2 production.

Discussion

Exaggerated responses to agonists of G protein–coupled receptors expressed on airway smooth muscle represent a central feature of human asthma. Although the core pathway linking receptor ligation to airway smooth muscle contraction has been well established, much remains unknown about how this core pathway is modulated and why this pathway is hyperresponsive in asthma. Interactions between integrins and the surrounding ECM have

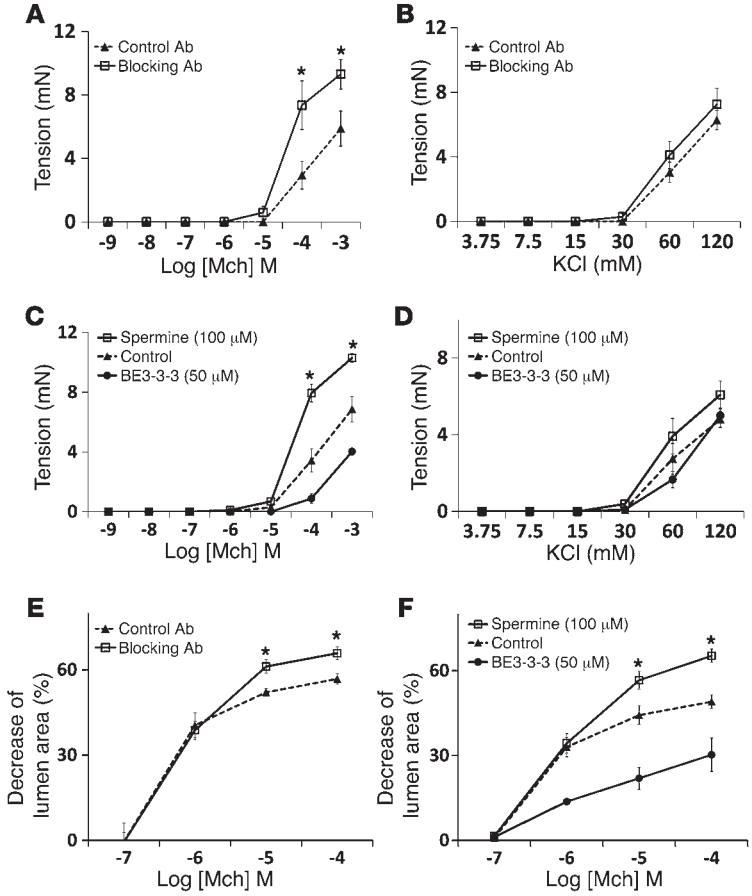

Figure 7
Blocking integrin $\alpha_9\beta_1$ enhances human airway narrowing and bronchial contraction. (**A** and **B**) Force generation in response to methacholine (**A**) or KCl (**B**) by human bronchial rings treated with mouse anti-human integrin $\alpha_9\beta_1$–blocking antibody (Y9A2; 10 μg/ml) or control antibody (10 μg/ml) for 24 hours. (**C** and **D**) Force generation in response to methacholine (**C**) or KCl (**D**) by bronchial rings treated with BE3-3-3 (50 μM) or spermine (100 μM) for 24 hours. (**E** and **F**) Airway contraction in human lung slices treated with anti-human integrin $\alpha_9\beta_1$–blocking antibody (Y9A2; 10 μg/ml) or control antibody (**E**) or with BE3-3-3 (50 μM) or spermine (100 μM) (**F**) for 24 hours. Data (mean ± SEM) represent 2 independent experiments with similar results. *$P < 0.01$.

been shown to regulate airway smooth muscle proliferation (34, 35) and to connect smooth muscle cells to the matrix, allowing contraction to be translated into the force generation required for airway narrowing (14). Here, we describe a role for ligation of integrin $\alpha_9\beta_1$ in preventing exaggerated contraction of airway smooth muscle, which we believe to be novel. Integrin-mediated prevention of smooth muscle contraction depends on the previously described association of the integrin α_9 cytoplasmic domain with SSAT and is caused by catabolism of higher-order polyamines (spermine and spermidine). A reduction in local concentrations of polyamines appears to decrease the contractile response to G protein–coupled receptor agonists by reducing the activity of the integrin-associated lipid kinase PIP5K1γ, which reduces the concentration of available PIP2 and thus inhibits IP_3-mediated calcium release from the smooth muscle SR (Figure 11). These conclusions are supported by our findings that exogenous PIP2 enhanced contraction only in control airway smooth muscle and that overexpression of WT PIP5K1γ, but not a kinase-dead version or a version that cannot localize to integrins, also enhanced contraction only in smooth muscle containing functional, ligated integrin $\alpha_9\beta_1$.

Integrin $\alpha_9\beta_1$ is highly expressed in airway smooth muscle. This integrin has been shown to interact with a wide variety of ligands, including the endothelial counter receptor VCAM-1 (36), tenascin C (37), osteopontin (38, 39), cellular fibronectin (40), several members of the a disintegrin and metalloprotease (ADAM) family (41–43), coagulation factor XIII (44), tissue transglumatinase (44), VEGFA (45, 46), VEGFC and VEGFD (47), and von Willebrand factor (44). Our current findings suggest that integrin $\alpha_9\beta_1$ ligation is required for inhibition of airway smooth muscle contraction, since blocking antibody that inhibits interactions with ligands was as effective as KO or knockdown of the integrin in enhancing airway smooth muscle contraction. However, given the large number of potential ligands, we have not attempted here to identify the relevant ligand on or near airway smooth muscle.

We have previously shown that another effect of integrin $\alpha_9\beta_1$, accelerated cell migration, depends on the interaction between the integrin α_9 cytoplasmic domain and SSAT (24, 25). SSAT is the rate-limiting step in catabolism of higher-order polyamines (48), which converts spermine to spermidine and then spermidine to putrescine. Because SSAT is rapidly ubiquitinated and degraded in cells, for in vitro experiments it was necessary to use the polyamine analog BE3-3-3, which binds to SSAT and prevents its degradation. By preventing SSAT degradation, this drug effectively enhances SSAT activity, and it has thus proven a useful tool to probe SSAT-mediated effects in cells. In this study, we found that airway narrowing in lung slices and force generation by tracheal rings were decreased by BE3-3-3 treatment only in tissues in which integrin α_9 was expressed and functional; BE3-3-3 had no effect on tissues of $\alpha_9$smKO mice or animals treated with integrin $\alpha_9\beta_1$–blocking antibody. Furthermore, exogenous spermine also enhanced airway narrowing and force generation only in tissues in which integrin α_9 was expressed and functional on airway smooth muscle. Together, these results strongly suggest that integrin $\alpha_9\beta_1$ normally inhibits airway smooth muscle contraction through interaction with SSAT and local breakdown of higher-order polyamines.

The 2 best-characterized cytosolic effects of spermidine and spermine that are not shared by putrescine are inward rectification of inwardly rectifying potassium (Kir) channels (49, 50) and dramatic enhancement of PIP5K1γ activity (31, 51). We have previously shown that integrin $\alpha_9\beta_1$–mediated enhancement of cell migration is caused by altered rectification of a specific Kir channel, Kir4.2 (25), and have found that Kir4.2 is also the major Kir channel expressed in airway smooth muscle (our unpublished observations). However, we found that inhibiting Kir channels by barium chloride had no effect on force generation by tracheal rings or lung slices (our unpublished observations). PIP5K1γ is the major source of PIP2 in airway smooth muscle cells (31). Conversion of PIP2 to IP_3 is a critical step in the pathway by which G protein–coupled receptor agonists induced calcium efflux from the SR, an important step regulating smooth muscle contraction. We found that increased cellular PIP2 concentration or increased PIP5K1γ kinase

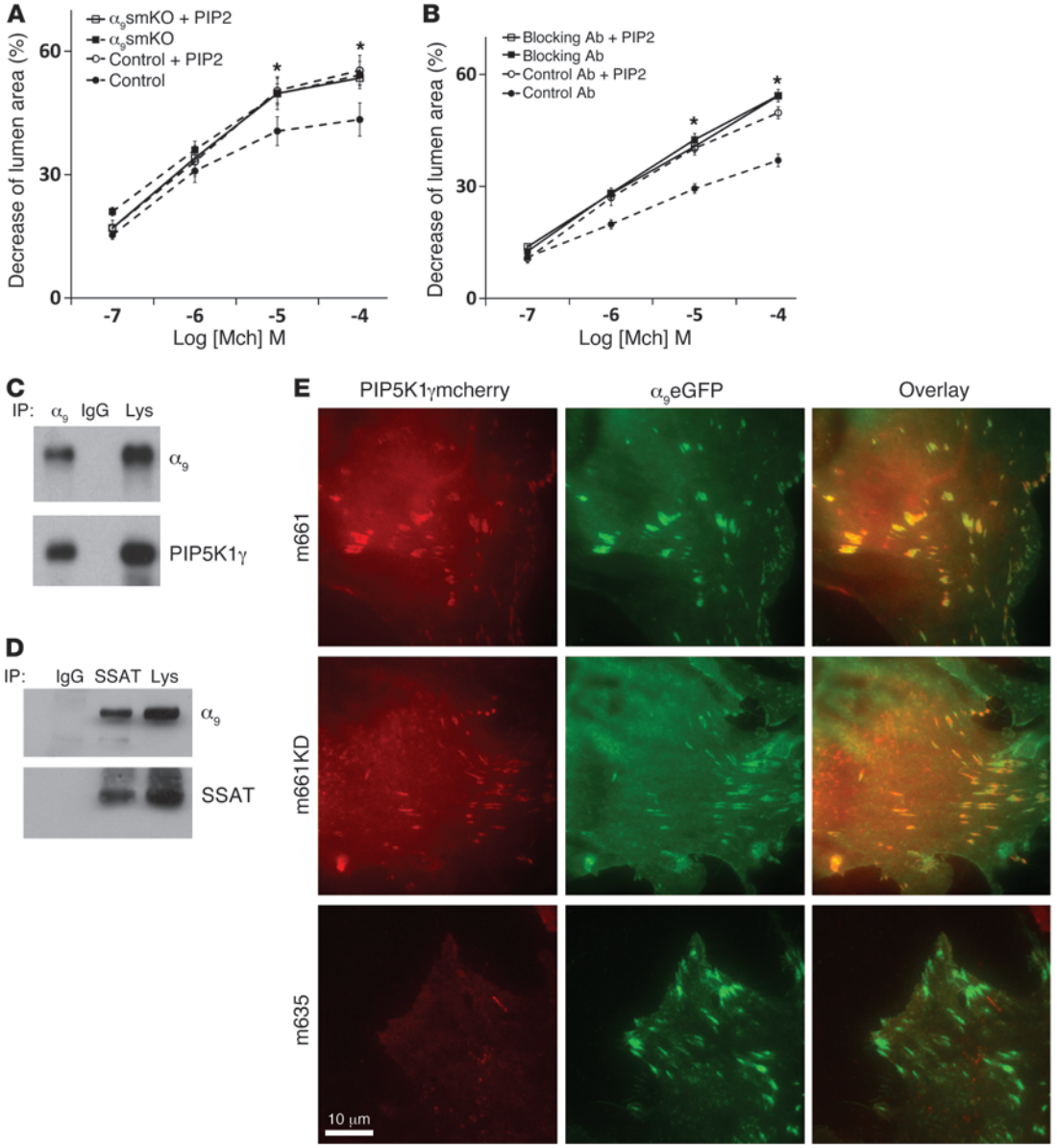

Figure 8

Interaction between PIP5K1γ and integrin $\alpha_9\beta_1$ in airway smooth muscle cells. (**A** and **B**) Airway narrowing was measured on lung slices from control and $\alpha_9$smKO mice, either (**A**) untreated or (**B**) treated with control or blocking antibody, that were also treated with either cell-permeable diC16-PIP2 and carrier 3 (the lipid carrier) or carrier 3 alone. *$P < 0.01$. (**C**) Co-IP of integrin $\alpha_9\beta_1$ and PIP5K1γ. Lysate from mouse tracheal tissue was subjected to IP by anti–integrin α_9 or rabbit IgG control followed by protein G–sepharose. Precipitated proteins (or cell lysates; Lys) were detected with anti–integrin α_9 and anti-PIP5K1γ. (**D**) Co-IP of integrin $\alpha_9\beta_1$ and SSAT. Mouse tracheal tissues were treated with BE3-3-3 (50 μM) for 24 hours before lysis. Lysates were subjected to IP by anti-SSAT or rabbit IgG control and detected with anti–integrin α_9 and SSAT. (**E**) Mouse airway smooth muscle cells were cotransfected by integrin α_9–EGFP (α_9eGFP) and PIP5K1γ-mcherry fusion cDNA (m661, full-length PIP5K1γ; m661KD, kinase-dead mutation; m635, truncated PIP5K1γ lacking the 26 amino acids that interact with talin). Scale bar: 10 μm.

activity reversed the inhibitory effects of integrin $\alpha_9\beta_1$. Furthermore, the absence of this integrin enhanced the frequency of calcium oscillations in airway smooth muscle, and this effect was inhibited by BE3-3-3 and enhanced by spermine only in smooth muscle that expressed integrin α_9. These data support the hypothesis that integrin $\alpha_9\beta_1$ and SSAT prevent airway narrowing at least in part through modulation of PIP5K1γ activity and PIP2 generation, and that these effects are mediated by enhanced calcium release from intracellular stores. The absence of any effects of integrin α_9 loss on the contractile response to KCl, which bypasses all these steps by inducing influx of extracellular calcium through voltage-gated calcium channels, provided further support for this interpretation.

PIP2 also plays an important role in linking actin to integrin-mediated adhesion sites, a key step in agonist-induced force generation by airway smooth muscle (52, 53). However, as noted above, loss of integrin α_9 on airway smooth muscle specifically

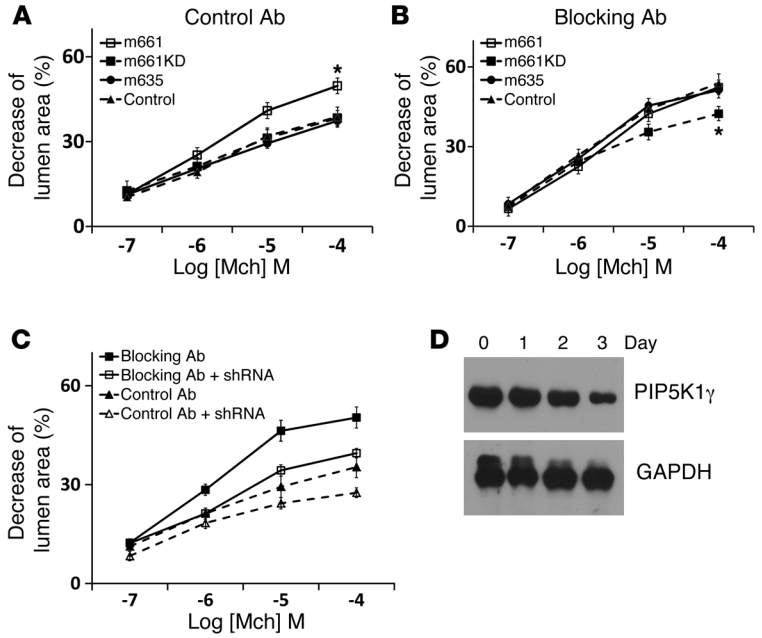

Figure 9
Dependence of effect of airway smooth muscle integrin $\alpha_9\beta_1$ on PIP5K1γ. (**A** and **B**) Airway narrowing in lung slices treated with control antibody (**A**) or blocking antibody (**B**) and infected by adenovirus expressing full-length, truncated, or kinase-dead PIP5K1γ. (**C**) Airway narrowing in lung slices treated with control antibody or blocking antibody and infected by adenovirus expressing shRNA targeting mouse PIP5K1γ. (**D**) Decreased PIP5K1γ expression in mouse lung slices after infection with adenovirus expressing shRNA targeting PIP5K1γ. Mouse lung slices were incubated with shRNA-expressing adenovirus for 0, 1, 2, or 3 days. Data (mean ± SEM) represent 2 independent experiments with similar results. *$P < 0.01$.

inhibited responses to G protein–coupled receptor ligation, with no effect on contractile responses to smooth muscle depolarization by KCl. If integrin $\alpha_9\beta_1$ was principally modulating smooth muscle contraction by enhancing interactions between actin and other anchoring integrins, we would have also expected effects on KCl-induced contraction. However, we cannot exclude some contribution of PIP2's effects on integrin anchoring as an amplifier of the inhibitory response we describe herein.

It is tempting to speculate that the pathway we describe could have relevance to the exaggerated airway narrowing that characterizes human asthma. For example, our results would predict that genetic or acquired defects in integrin $\alpha_9\beta_1$, its relevant ligands, or SSAT could result in functionally important airway hyperresponsiveness in humans. Furthermore, these results suggest that stabilization of SSAT or inhibition of PIP5K1γ could represent novel therapies for prevention of airway smooth muscle contraction in asthma.

Methods

Reagents. Polyclonal antiserum was raised in rabbits against the mouse integrin α_9 cytoplasmic domain peptide NRKENEDGWDWVQKNQ and affinity purified. Hamster monoclonal antibody 55A2C against murine integrin α_9 was previously described (54). Human integrin $\alpha_9\beta_1$–blocking antibody Y9A2 was generated in our laboratory (55). Both blocking antibodies bind the extracellular domains of the integrin, as determined by flow cytometry, and block ligand binding, as determined by cell adhesion assays (36, 54, 56). BE3-3-3 was from TOCRIS. Adenoviruses expressing GFP or Cre recombinase were gifts from L. Wu (UCLA, Los Angeles, California, USA). diC16-PIP2 and carrier vehicle were from Echelon Biosciences Inc. Mouse monoclonal antibody against PIP5K1γ was from BD Biosciences. Mouse monoclonal antibody against α-SMA was from Sigma-Aldrich. An integrin $\alpha_9\beta_1$–specific mutant form of the third fibronectin type III repeat in tenascin-C(TNfn3RAA) was previously described (57).

Mouse lines. *Itga9*^{fl} (18), *Gt(ROSA)26Sor*$^{tm4(ACTB-tdTomato,-EGFP)Luo}$/J (20), and (tetO)7-Cre (19) mouse lines have been described previously. α-sm-rTTA mice were provided by M. Shipley (Washington University School of Medicine, St. Louis, Missouri, USA). Mice were maintained on a C57BL/6 background and housed at the UCSF animal care facility.

Integrin α_9 reporter mouse generation. A knockin ES cell clone was obtained from Knock-Out Mouse Project (www.komp.org; project no. VG12163). LacZ cDNA was inserted downstream of the endogenous *Itga9* promoter.

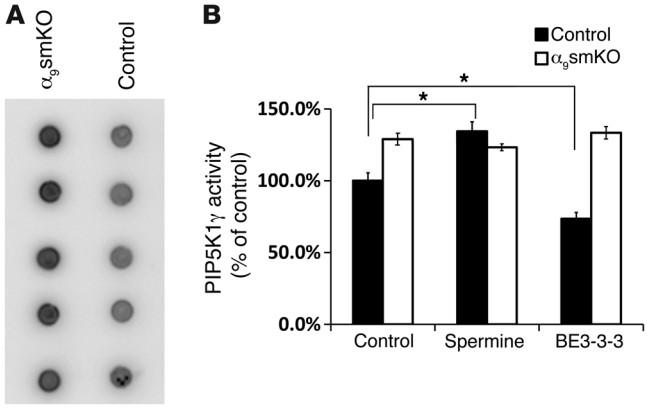

Figure 10
PIP5K1γ activities are regulated by integrin $\alpha_9\beta_1$ and polyamines. (**A**) Mouse tracheal smooth muscle tissues (5 mice per group) were lysed, PIP5K1γ kinase was subjected to IP by anti-PIP5K1γ antibody, and kinase activity was calculated as the transfer of [γ-^{32}P] to PI4P from [γ-^{32}P] ATP. Developed blots for all samples in each group are shown. (**B**) Mouse tracheal smooth muscle tissues were incubated with or without spermine (100 μM) or BE3-3-3 (50 μM) for 24 hours. PIP5K1γ activity is expressed as a percentage of control. Data are mean ± SEM ($n = 5$). *$P < 0.01$.

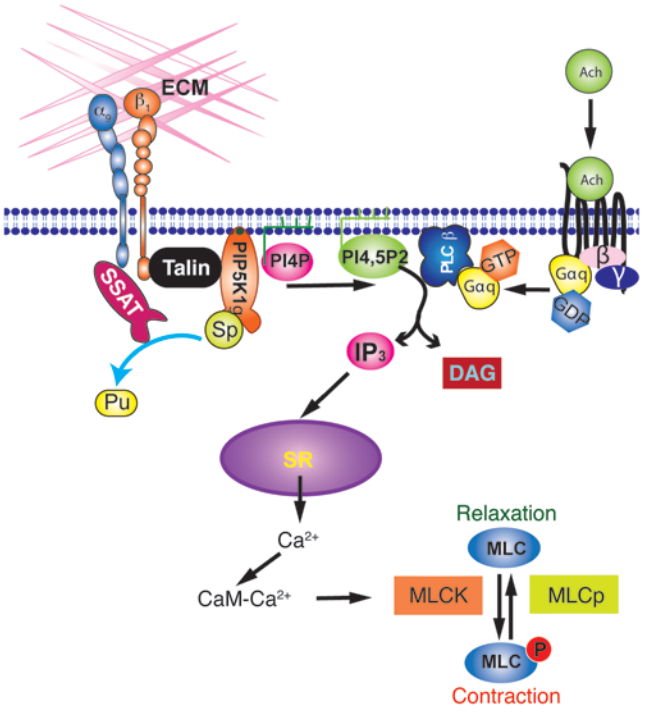

Figure 11
Integrin $\alpha_9\beta_1$ inhibits airway smooth muscle contraction by interacting with SSAT and regulating PIP5K1γ kinase activity. CaM, calmodulin; DAG, diacylglycerol; MLCK, MLC kinase; Pu, putrescine.

ES cell blastocyst injection was performed in the transgenic mouse core of the Gladstone Research Institute, germline transmission was confirmed, and heterozygous reporter mice were used to obtain lung sections.

Immunostaining. Fresh mouse lungs were inflated by intratracheal injection with cold PBS containing 15% sucrose mixed with ornithine-carbamyltransferase (OCT), then embedded in OCT. Mouse trachea was embedded in OCT directly. Cryostat sections (5 μm) were cut onto glass slides and stored at −80°C after 1 hour air drying. For immunofluorescent staining, tissues were fixed in cold acetone for 5 minutes at –20°C. Nonspecific binding was blocked by incubation with 5% goat serum in PBS for 30 minutes at room temperature, followed by overnight incubation with rabbit anti–integrin α_9 at 4°C. Samples were visualized with Alexa Fluor 488 goat anti-rabbit antiserum (Invitrogen).

Lungs from *LacZ* knockin mice were inflated by 4% paraformaldehyde in PBS for 1 hour at 4°C. Fixed tissues were transferred to PBS containing 20% sucrose overnight (4°C), after which they were embedded in OCT. 10-μm sections were cut and incubated with X-gal (1 mg/ml; Invitrogen) at 37°C for 12 hours. After staining, sections were washed with PBS, then incubated with rat anti-mouse E-cadherin (R&D Systems) and Cy3-conjugated anti-mouse α-SMA (Sigma-Aldrich) followed by Alexa Fluor 488 goat anti-rat (Invitrogen).

Airway smooth muscle culture. Primary cultures of murine airway smooth muscle cells were established from tracheal explants of $\alpha_9$smKO mice and WT controls. The trachea was removed and placed on a dish containing HBSS supplemented with antibiotic solution. Tracheal segments were dissected into 2- to 3-mm squares and placed in a 6-well plate. After adherence, DMEM with 20% FCS was added to cover the explants. Explanted tracheas were subsequently removed when there was local confluence of the outgrowth of smooth muscle cells. The purity of airway smooth muscle cells was confirmed by anti–α-SMA staining.

Measurement of airway response to acetylcholine. WT and $\alpha_9$smKO mice (8–10 weeks old) were anesthetized with ketamine/xyalazine, attached to a rodent ventilator and pulmonary mechanics analyzer (FlexiVent; SIRAQ Inc.), and ventilated at a tidal volume of 9 ml/kg, a frequency of 150 breaths/minute, and 2 cmH_2O positive end-expiratory pressure. Mice were paralyzed with pancuronium (0.1 mg/kg intraperitoneally). A 27-gauge needle was placed in the tail vein, and measurements of airway mechanics were made continuously using the forced oscillation technique. Mice were given increasing doses of acetylcholine (0.03, 0.1, 0.3, 1, and 3 μg/g body weight) administered through the tail vein to generate a concentration-response (58).

Measurement of lung static compliance. WT and $\alpha_9$smKO mice were anesthetized with ketamine (100 mg/kg), xylazine (10 mg/kg), and acepromazine (2–3 mg/kg). A tracheostomy was performed, and a tubing adaptor (20 gauge) was used to cannulate the trachea. The mice were then attached to a rodent ventilator and pulmonary mechanics analyzer (FlexiVent; SIRAQ Inc.) and ventilated at a tidal volume of 9 ml/kg, a frequency of 150 breaths/minute, and 2 cmH_2O positive end-expiratory pressure. The animals were then paralyzed with pancuronium (0.1 mg/kg intraperitoneally) and allowed to adjust to the ventilator. Static compliance was calculated from quasistatic pressure/volume curves that were generated by stepwise inflation and deflation of the lungs.

Mouse lung slices. Murine lung slices were prepared as described by Bai and Sanderson (21) from 6- to 10-week-old mice on the C57BL/6 background. After the chest cavity was opened, the lungs were inflated with 1.0 ml warm (37°C) 2% low-melting agarose through a tracheal catheter, and 0.2 ml air was injected to flush the agarose out of the airways. After gelling of the agarose in the whole lung by cooling to 4°C, a single lobe was removed and cut into serial sections of 140 μm thickness with a vibratome (VT1000S; Leica) at 4°C. Slices were maintained in DMEM supplemented with antibiotics at 37°C and 10% CO_2 for up to 3 days.

Human lung slices. Human lung slices were prepared by the previously described protocol (59) modified in our lab. Human lobectomy samples (obtained from explanted lungs during lung transplantation) were warmed in a 37°C water bath, then inflated with a warm agarose solution (4% in PBS, 37°C) via the mainstem bronchus. To solidify the agarose, the tissue was cooled with ice for 30 minutes. 400-μm slices were prepared with a vibratome (as above) from tissue sections containing visible airways. The viability of the slices was confirmed by active cilia beating in the airways.

Measurement of airway contraction. Lung slices were maintained overnight in DMEM with or without polyamines, BE3-3-3, and/or antibodies. 2 lung slices were placed in a 6-well plate with 3.0 ml DMEM and held by a Slice Anchor (SHD-22L/10; Warner Instruments). The whole lung slice was imaged (area scan) with a Leica DM6000 inverted microscope using a ×5 objective. The microscope was equipped with a temperature chamber maintained at 37°C. Multiple airways in 1 lung slice were recorded in time lapse (1 frame/min) for 10 minutes. Methacholine was added after the first recording. The lumen area of the airway was measured by ImagePro software (Media Cybernetics Inc.).

Measurements of intracellular Ca^{2+} oscillation. The protocol was modified from that of Bai et al. (21). Briefly, lung slices were labeled by Oregon green 488 BAPTA-AM (20 μM in HBSS containing 0.1% Pluronic F-127 and 100 μM sulfobromophthalein) for 45 minutes at 30°C and de-esterified for 30 minutes at 30°C in HBSS containing 100 μM sulfobromophthalein. Lung slices were placed in coverglass chambers (Lab-Tek) and immobilized by Slice Anchor. Fluorescence imaging was performed with a Nikon spinning-disk confocal microscope at 20 frames/s using a ×10 Nikon objective. Changes in fluorescence intensity from selected regions of interest (5 × 5 pixels) were analyzed by ImageJ software.

Tracheal ring contraction. Tracheal ring segments approximately 3 mm in length were suspended in a 15-ml organ bath by 2 stainless-steel wires (0.2 mm diameter) passed through the lumen. One wire was fixed to the organ

bath, whereas the other was connected to a force-displacement transducer (FT03; Grass Instrument Co.) for the measurement of isometric force. A resting tension of 0.5 g was applied, and rings were equilibrated for 45 minutes. The buffer solution, containing modified Krebs-Henseleit solution (117.5 mM NaCl, 5.6 mM KCl, 2.5 mM $CaCl_2$, 1.18 mM $MgSO_4$, 25 mM $NaHCO_3$, 1.28 mM NaH_2PO_4, and 5.55 mM glucose), was maintained at 37°C and oxygenated with 95% O_2 and 5% CO_2. In some experiments, rings were incubated with antibodies or adenovirus in a 37°C incubator with 5% CO_2 for 24 hours prior to study. Rings were first contracted by 60 mM KCl, and only those that could generate more than 2.5 mN tension were used for experiments. Rings were washed and re-equilibrated, and contractile response was then evaluated with increasing concentrations of methacholine (10^{-9} to 10^{-4} M) or KCl (3.75 to 60 mM). To evaluate whether integrin $\alpha_9\beta_1$ modulates airway contraction through effects on epithelial cells, we completely removed epithelium in some rings by gentle rubbing with roughened PE-10 tubing. Epithelial removal was confirmed for each individual ring by microscopic observation of H&E-stained sections.

Isolated human bronchi. Bronchi with diameters between 3 and 8 mm were dissected free of lung and connective tissue and cut into 3- to 4-mm-thick rings. The tissues were then incubated overnight at 37°C in DMEM with antibodies, polyamines, or BE3-3-3 and used for contraction in 15-ml organ baths as described above.

Adenovirus production. Clones for mcherry-tagged full-length murine PIP5K1γ, kinase-dead mutant, and truncated mutant lacking the 26 amino acids that interact with talin were provided by R.A. Anderson (University of Wisconsin–Madison, Madison, Wisconsin, USA). cDNAs were subcloned into pshuttle-CMV vector. Adenoviruses were then produced and amplified using the AdEasy XL Adenoviral System (Agilent Technologies). For infection, 10^8 pfu viruses were used for each lung slice.

shRNA-mediated knockdown of mouse PIP5K1γ. shRNA was designed using pSicoOligomaker 1.5 (http://web.mit.edu/jacks-lab/protocols/pSico.html). shRNAs were cloned into the lentiviral vector pSICOR and verified by sequencing. Lentiviruses were produced in HEK 293T cells and used to infect mouse embryonic fibroblasts. Infected cells were enriched by fluorescence-activated cell sorting and selected for high EGFP expression. The efficiency of shRNA-mediated knockdown was evaluated by Western blot. shRNA 2045 (targeting 5′-GAAGACCTGCAGAAGATAA-3′) knocked down PIP5K1γ protein more than 90% (Supplemental Figure 4). shRNA 1791 (targeting 5′-GAGAGGATGTGCAGTATGA-3′) had no effect on PIP5K1γ expression and was used as control shRNA. To knock down PIP5K1γ in mouse lung slices, the shRNA expression cassette was cloned into the pShuttle vector, and adenovirus was generated as described above.

Fluorescent protein expression and microscopy. Mouse airway smooth muscle cells were prepared as described above. Cells within passage 4 were serum starved for 24 hours before transfection. Fluorescent protein–tagged human integrin α_9 and mouse PIP5K1γ cDNAs were cotransfected by Nucleofector (Basic Smooth Muscle Cells [SMC] Nucleofector Kit; Lonza). Cells were plated on Tnfn3RAA-coated coverglass chambers and imaged 24 hours later on a total internal reflection fluorescence microscope (TE2000E; Nikon), using a Photometrics Cascade II EM CCD camera and Nikon NIS Elements software (all stationed at the Nikon Imaging Center at UCSF).

PIP5K1γ kinase activity assay. Mouse tracheal smooth muscle tissues were lysed in IP buffer (50 mM Tris-HCl, pH 7.5; 150 mM NaCl; 1.0% Triton X-100; 5.0 mM NaF; 2 mM Na_3VO_4; 1 mM EDTA; 0.1 mM EGTA; 10% glycerol; and proteinase inhibitor cocktail), centrifuged, and incubated with protein A–sepharose and rabbit anti-PIP5K1γ antibody (ab109192; Abcam) at 4°C overnight. Sepharose were then washed 3 times with IP buffer. PIP5K1γ kinase activity was assayed following a previously described method for lipid kinases (60). Kinase activity was assayed at room temperature in a 40-μl final reaction volume consisting of 20 μl buffer substrate solution and 20 μl IP protein. Reaction conditions consisted of 30 mM Tris (pH 7.4), 1.2 mM $MgCl_2$, 0.3 mg/ml BSA, 60 μM dithiothreitol, 0.06 mg/ml PI4P/DOPS (1:1; Avanti Polar Lipids), 3.5 μM ATP, and 22 μCi [γ-^{32}P] ATP (Perkin Elmer). To prepare lipids, 1 mg DOPS powder was suspended in 1 ml water and sonicated in a water bath sonicator for 20 seconds to create a 1-mg/ml solution of DOPS carrier lipid. 1 mg solid PI4P was then suspended in the DOPS solution and sonicated in a water bath sonicator for 20 seconds to generate 1 mg/ml PI4P/DOPS lipid vesicles at a 1:1 ratio. The kinase reaction was started by the addition of ATP and was terminated after 2 hours by spotting 4 μl of the reaction onto 0.2 μm nitrocellulose membrane. When spotting was complete, the membrane was dried under a heat lamp for 5 minutes. The membrane was washed once with 200 ml of 1% phosphoric acid in 1 M NaCl for 30 seconds, followed by 4 washes for 5 minutes, and finally for an additional 3 hours. The membrane was dried for 1 hour, exposed for 43 hours on a phosphor screen, and scanned using the Typhoon (GE Healthcare). The intensity of each spot was quantified by densitometry using SPOT (60). PIP5K1γ activity was normalized by protein concentrations in tissue lysates and expressed as a percentage of WT tracheal tissue activity.

Statistics. All error bars denote SEM. Results were analyzed with SigmaStat software using 1-way ANOVA followed by Newman-Keuls test. A P value less than 0.05 was considered significant.

Study approval. All studies in mice were approved by the institutional review board of UCSF. Written informed consent was obtained from all subjects, and the study was approved by the UCSF Committee on Human Research. Human lung tissues were obtained from explanted lung during lung transplantation.

Acknowledgments

The authors thank Lily Wu for the Cre adenovirus; Emily Thornton, Matthew F. Krummel, and Nan Tang (UCSF, San Francisco, California, USA) for assistance in preparing mouse lung slices; Mary Ann Stepp (George Washington University, Washington, DC, USA) for help with preparing rabbit polyclonal antibody against integrin α_9; Mary B. Engler for assistance with setting up the muscle bath; Junli Zhang for ES cell blastocyst injection; Chong Park for ES cell expansion and characterization; Anthony E. Pegg (Pennsylvania State University College of Medicine, Hershey, Pennsylvania, USA) for valuable advice about polyamines; and Kurt Thorn, Sebastian Peck, and UCSF Nikon Imaging Center for assistance with imaging. This work was supported by NIH grants HL102292, HL53949, and AI077439 (to D. Sheppard) and by the UCSF Strategic Asthma Basic Research Center (SABRE).

Received for publication August 8, 2011, and accepted in revised form May 30, 2012.

Address correspondence to: Dean Sheppard, Lung Biology Center, University of California San Francisco, Box 2922, San Francisco, California 94143-2922, USA. Phone: 415.514.4269; Fax: 415.514.4278; E-mail: dean.sheppard@ucsf.edu.

1. Hynes RO. Integrins: bidirectional, allosteric signaling machines. *Cell*. 2002;110(6):673–687.
2. Hynes RO. Integrins: versatility, modulation, and signaling in cell adhesion. *Cell*. 1992;69(1):11–25.
3. Clark EA, Brugge JS. Integrins and signal transduction pathways: the road taken. *Science*. 1995; 268(5208):233–239.
4. Chen C, Sheppard D. Identification and molecular characterization of multiple phenotypes in integrin knockout mice. *Methods Enzymol*. 2007;426:291–305.
5. Hynes RO, Bader BL. Targeted mutations in integrins and their ligands: their implications for vascular biology. *Thromb Haemost*. 1997;78(1):83–87.
6. Hynes RO, Bader BL, Hodivala-Dilke K. Integrins in vascular development. *Braz J Med Biol Res*.

1999;32(5):501–510.
7. Sheppard D. In vivo functions of integrins: lessons from null mutations in mice. *Matrix Biol*. 2000; 19(3):203–209.
8. Nakajima H, Sano H, Nishimura T, Yoshida S, Iwamoto I. Role of vascular cell adhesion molecule 1/very late activation antigen 4 and intercellular adhesion molecule 1/lymphocyte function-associated antigen 1 interactions in antigen-induced eosinophil and T cell recruitment into the tissue. *J Exp Med*. 1994;179(4):1145–1154.
9. Pretolani M, Ruffie C, Lapa e Silva JR, Joseph D, Lobb RR, Vargaftig BB. Antibody to very late activation antigen 4 prevents antigen-induced bronchial hyperreactivity and cellular infiltration in the guinea pig airways. *J Exp Med*. 1994;180(3):795–805.
10. Richards IM, et al. Role of very late activation antigen-4 in the antigen-induced accumulation of eosinophils and lymphocytes in the lungs and airway lumen of sensitized brown Norway rats. *Am J Respir Cell Mol Biol*. 1996;15(2):172–183.
11. Wegner CD, Gundel RH, Reilly P, Haynes N, Letts LG, Rothlein R. Intercellular adhesion molecule-1 (ICAM-1) in the pathogenesis of asthma. *Science*. 1990;247(4941):456–459.
12. Sugimoto K, et al. The alphavbeta6 integrin modulates airway hyperresponsiveness in mice by regulating intraepithelial mast cells. *J Clin Invest*. 2012; 122(2):748–758.
13. Kudo M, et al. IL-17A produced by alphabeta T cells drives airway hyper-responsiveness in mice and enhances mouse and human airway smooth muscle contraction. *Nat Med*. 2012;18(4):547–554.
14. Zhang W, Gunst SJ. Interactions of airway smooth muscle cells with their tissue matrix: implications for contraction. *Proc Am Thorac Soc*. 2008;5(1):32–39.
15. Weiss LA, et al. Variation in ITGB3 is associated with asthma and sensitization to mold allergen in four populations. *Am J Respir Crit Care Med*. 2005;172(1):67–73.
16. Van Eerdewegh P, et al. Association of the ADAM33 gene with asthma and bronchial hyperresponsiveness. *Nature*. 2002;418(6896):426–430.
17. Huang XZ, et al. Fatal bilateral chylothorax in mice lacking the integrin alpha9beta1. *Mol Cell Biol*. 2000;20(14):5208–5215.
18. Singh P, Chen C, Pal-Ghosh S, Stepp MA, Sheppard D, Van De Water L. Loss of integrin alpha9beta1 results in defects in proliferation, causing poor re-epithelialization during cutaneous wound healing. *J Invest Dermatol*. 2009;129(1):217–228.
19. Perl AK, Wert SE, Nagy A, Lobe CG, Whitsett JA. Early restriction of peripheral and proximal cell lineages during formation of the lung. *Proc Natl Acad Sci U S A*. 2002;99(16):10482–10487.
20. Muzumdar MD, Tasic B, Miyamichi K, Li L, Luo L. A global double-fluorescent Cre reporter mouse. *Genesis*. 2007;45(9):593–605.
21. Bai Y, Sanderson MJ. Modulation of the Ca2+ sensitivity of airway smooth muscle cells in murine lung slices. *Am J Physiol Lung Cell Mol Physiol*. 2006; 291(2):L208–L221.
22. Yamamoto N, et al. Essential role of the cryptic epitope SLAYGLR within osteopontin in a murine model of rheumatoid arthritis. *J Clin Invest*. 2003; 112(2):181–188.
23. Tolloczko B, Jia YL, Martin JG. Serotonin-evoked calcium transients in airway smooth muscle cells. *Am J Physiol*. 1995;269(2 pt 1):L234–L240.
24. Chen C, Young BA, Coleman CS, Pegg AE, Sheppard D. Spermidine/spermine N1-acetyltransferase specifically binds to the integrin alpha9 subunit cytoplasmic domain and enhances cell migration. *J Cell Biol*. 2004;167(1):161–170.
25. deHart GW, Jin T, McCloskey DE, Pegg AE, Sheppard D. The alpha9beta1 integrin enhances cell migration by polyamine-mediated modulation of an inward-rectifier potassium channel. *Proc Natl Acad Sci U S A*. 2008;105(20):7188–7193.
26. Coleman CS, Pegg AE. Polyamine analogues inhibit the ubiquitination of spermidine/spermine N1-acetyltransferase and prevent its targeting to the proteasome for degradation. *Biochem J*. 2001;358(pt 1):137–145.
27. Holtta E. Oxidation of spermidine and spermine in rat liver: purification and properties of polyamine oxidase. *Biochemistry*. 1977;16(1):91–100.
28. Perez JF, Sanderson MJ. The frequency of calcium oscillations induced by 5-HT, ACH, and KCl determine the contraction of smooth muscle cells of intrapulmonary bronchioles. *J Gen Physiol*. 2005; 125(6):535–553.
29. Dillon PF, Aksoy MO, Driska SP, Murphy RA. Myosin phosphorylation and the cross-bridge cycle in arterial smooth muscle. *Science*. 1981;211(4481):495–497.
30. Doughman RL, Firestone AJ, Anderson RA. Phosphatidylinositol phosphate kinases put PI4,5P(2) in its place. *J Membr Biol*. 2003;194(2):77–89.
31. Chen H, Baron CB, Griffiths T 2nd, Greeley P, Coburn RF. Effects of polyamines and calcium and sodium ions on smooth muscle cytoskeleton-associated phosphatidylinositol (4)-phosphate 5-kinase. *J Cell Physiol*. 1998;177(1):161–173.
32. Di Paolo G, et al. Recruitment and regulation of phosphatidylinositol phosphate kinase type 1 gamma by the FERM domain of talin. *Nature*. 2002; 420(6911):85–89.
33. Ling K, Doughman RL, Firestone AJ, Bunce MW, Anderson RA. Type I gamma phosphatidylinositol phosphate kinase targets and regulates focal adhesions. *Nature*. 2002;420(6911):89–93.
34. Dekkers BG, Schaafsma D, Nelemans SA, Zaagsma J, Meurs H. Extracellular matrix proteins differentially regulate airway smooth muscle phenotype and function. *Am J Physiol Lung Cell Mol Physiol*. 2007;292(6):L1405–L1413.
35. Hirst SJ, et al. Proliferative aspects of airway smooth muscle. *J Allergy Clin Immunol*. 2004; 114(2 suppl):S2–S17.
36. Taooka Y, Chen J, Yednock T, Sheppard D. The integrin alpha9beta1 mediates adhesion to activated endothelial cells and transendothelial neutrophil migration through interaction with vascular cell adhesion molecule-1. *J Cell Biol*. 1999; 145(2):413–420.
37. Yokosaki Y, et al. The integrin alpha 9 beta 1 mediates cell attachment to a non-RGD site in the third fibronectin type III repeat of tenascin. *J Biol Chem*. 1994;269(43):26691–26696.
38. Smith LL, et al. Osteopontin N-terminal domain contains a cryptic adhesive sequence recognized by alpha9beta1 integrin. *J Biol Chem*. 1996; 271(45):28485–28491.
39. Yokosaki Y, et al. The integrin alpha(9)beta(1) binds to a novel recognition sequence (SVVYGLR) in the thrombin-cleaved amino-terminal fragment of osteopontin. *J Biol Chem*. 1999;274(51):36328–36334.
40. Liao YF, Gotwals PJ, Koteliansky VE, Sheppard D, Van De Water L. The EIIIA segment of fibronectin is a ligand for integrins alpha 9beta 1 and alpha 4beta 1 providing a novel mechanism for regulating cell adhesion by alternative splicing. *J Biol Chem*. 2002;277(17):14467–14474.
41. Eto K, et al. Functional classification of ADAMs based on a conserved motif for binding to integrin alpha 9beta 1: implications for sperm-egg binding and other cell interactions. *J Biol Chem*. 2002; 277(20):17804–17810.
42. Tomczuk M, et al. Role of multiple beta1 integrins in cell adhesion to the disintegrin domains of ADAMs 2 and 3. *Exp Cell Res*. 2003;290(1):68–81.
43. Bridges LC, Sheppard D, Bowditch RD. ADAM disintegrin-like domain recognition by the lymphocyte integrins alpha4beta1 and alpha4beta7. *Biochem J*. 2005;387(pt 1):101–108.
44. Takahashi H, et al. Tissue transglutaminase, coagulation factor XIII, and the pro-polypeptide of von Willebrand factor are all ligands for the integrins alpha 9beta 1 and alpha 4beta 1. *J Biol Chem*. 2000; 275(31):23589–23595.
45. Oommen S, Gupta SK, Vlahakis NE. Vascular endothelial growth factor A (VEGF-A) induces endothelial and cancer cell migration through direct binding to integrin {alpha}9{beta}1: identification of a specific {alpha}9{beta}1 binding site. *J Biol Chem*. 2011;286(2):1083–1092.
46. Vlahakis NE, et al. Integrin alpha9beta1 directly binds to vascular endothelial growth factor (VEGF)-A and contributes to VEGF-A-induced angiogenesis. *J Biol Chem*. 2007;282(20):15187–15196.
47. Vlahakis NE, Young BA, Atakilit A, Sheppard D. The lymphangiogenic vascular endothelial growth factors VEGF-C and -D are ligands for the integrin alpha9beta1. *J Biol Chem*. 2005;280(6):4544–4552.
48. Casero RA Jr, Pegg AE. Spermidine/spermine N1-acetyltransferase--the turning point in polyamine metabolism. *FASEB J*. 1993;7(8):653–661.
49. Lopatin AN, Makhina EN, Nichols CG. Potassium channel block by cytoplasmic polyamines as the mechanism of intrinsic rectification. *Nature*. 1994;372(6504):366–369.
50. Kurata HT, et al. Molecular basis of inward rectification: polyamine interaction sites located by combined channel and ligand mutagenesis. *J Gen Physiol*. 2004;124(5):541–554.
51. Lundberg GA, Jergil B, Sundler R. Phosphatidylinositol-4-phosphate kinase from rat brain. Activation by polyamines and inhibition by phosphatidylinositol 4,5-bisphosphate. *Eur J Biochem*. 1986;161(2):257–262.
52. Raucher D, et al. Phosphatidylinositol 4,5-bisphosphate functions as a second messenger that regulates cytoskeleton-plasma membrane adhesion. *Cell*. 2000;100(2):221–228.
53. Chan MW, Arora PD, Bozavikov P, McCulloch CA. FAK, PIP5KIgamma and gelsolin cooperatively mediate force-induced expression of alpha-smooth muscle actin. *J Cell Sci*. 2009;122(pt 15):2769–2781.
54. Kanayama M, et al. Alpha9 integrin and its ligands constitute critical joint microenvironments for development of autoimmune arthritis. *J Immunol*. 2009;182(12):8015–8025.
55. Wang A, Yokosaki Y, Ferrando R, Balmes J, Sheppard D. Differential regulation of airway epithelial integrins by growth factors. *Am J Respir Cell Mol Biol*. 1996;15(5):664–672.
56. Kanayama M, et al. alpha9beta1 integrin-mediated signaling serves as an intrinsic regulator of pathogenic Th17 cell generation. *J Immunol*. 2011; 187(11):5851–5864.
57. Yokosaki Y, et al. Identification of the ligand binding site for the integrin alpha9 beta1 in the third fibronectin type III repeat of tenascin-C. *J Biol Chem*. 1998;273(19):11423–11428.
58. Chen C, Huang X, Sheppard D. ADAM33 is not essential for growth and development and does not modulate allergic asthma in mice. *Mol Cell Biol*. 2006;26(18):6950–6956.
59. Ressmeyer AR, et al. Human airway contraction and formoterol-induced relaxation is determined by Ca2+ oscillations and Ca2+ sensitivity. *Am J Respir Cell Mol Biol*. 2010;43(2):179–191.
60. Knight ZA, Feldman ME, Balla A, Balla T, Shokat KM. A membrane capture assay for lipid kinase activity. *Nat Protoc*. 2007;2(10):2459–2466.